Structure and Properties of Polyurethane Acrylate Prepolymers Based on Hydroxy-Terminated Polybutadiene

ISABELLE HENRY,[1] JEAN-PIERRE PASCAULT,[1] MOHAMED TAHA,[1] GÉRARD VIGIER,[2] JEAN-JACQUES FLAT[3]

[1] Laboratoire des Matériaux Macromoléculaires, UMR CNRS 5627, INSA Lyon Bât. 403-20, av. A. Einstein, 69621 Villeurbanne Cedex, France

[2] GEMPPM, UMR CNRS 5510-INSA Lyon Bât. 501-20, av. A. Einstein, 69621 Villeurbanne Cedex, France

[3] Elf-Atochem, CERDATO 27470 Serquigny, France

Received 8 June 2000; accepted 1 November 2000

ABSTRACT: Precursors of polyurethane acrylate based on hydroxy-terminated polybutadiene (HTPB) soft segments, different diisocyanate and hydroxy ethyl acrylate (HEA) as hard units, were synthesized in bulk or in solution in methyl methacrylate. During precursor synthesis (in bulk), microphase separation was observed by small-angle X-ray scattering (SAXS). Diffusing particles are around 50 Å in size and are assumed to be assembling of hard segments. From these morphologies, it can be deduced that some isocyanate groups were trapped/or buried in hard domains. At a larger scale, around millimeters, hard segment crystallites were observed. Properties such as molar masses, melting and glass-transition temperatures, and viscosities were correlated with precursor structure and morphology. © 2002 John Wiley & Sons, Inc. J Appl Polym Sci 83: 225–233, 2002

Key words: hydroxy-terminated polybutadiene; polyurethane acrylate; microphase separation; morphology; property

INTRODUCTION

Phase separation in polyurethane networks was observed by several investigators. It was demonstrated that because of their immiscibility, the hard segment units segregate from the soft segment units and form hard segment-rich microdomains (size about 50–150 Å).[1–7] Different techniques are commonly used for the characterization of the phase separated structure. Fourier transform infrared spectroscopy (FTIR) is used to observe hydrogen bonds created within hard domains, which are characteristic of microphase separation.[8–12] Differential scanning calorimetry (DSC) is a widely used tool to estimate the composition of soft and hard phases.[1,13,14] But the common technique used to observe formation of a two-phase structure is small-angle X-ray scattering (SAXS).[15–18] This method gives information on the morphology formed, micro-domain dimensions and degree of phase separation.[3–5,14–16] All these results could then be connected to mechanical behavior[3,19] and improve the understanding of polymer properties. Specific studies were devoted to the use of hydroxy-terminated polybutadiene (HTPB) as the soft segment and to its influence on polyurethane morphology.[2,6,13,20,21] The large degree of immiscibility observed is due

Correspondence to: M. Taha.
Present address: Université Jean Monnet, Laboratoire de Rhéologie des Matières Plastiques, 23, Rue du Dr. Paul Michelon 42023 Saint-Etienne Cedex 2, France.

Journal of Applied Polymer Science, Vol. 83, 225–233 (2002)

Table I Monomer Characteristics

Monomer	Abbreviation	Molar Mass (g/mol)	Functionality	Supplier
4,4′ Dicyclohexyl methane diisocyanate	H_{12}MDI	262.3	2	Bayer
m-Tetramethylxylene diisocyanate	mTMXDI	244.0	2	Cytec
Isophorone diisocyanate	IPDI	222.3	2	Aldrich
Toluene diisocyanate (80% 1,4; 20% 1,6)	TDI	174.2	2	Aldrich
Hydroxy-terminated polybutadiene	HTPB	2830[a]	2.50[a]	Elf Atochem PolyBd®
		7190[b]	2.93[b]	R45HT
2-Hydroxyethyl acrylate	HEA	116.1	1	Elf Atochem
Methyl methacrylate	MMA	100.1		Aldrich
Dibutyltin dilaurate	DBTL	631.56		Aldrich
Hydroquinone	HQ	110.11		Aldrich

[a] $\overline{M_n}$ or $\overline{F_{n_{OH}}}$.
[b] $\overline{M_w}$ or $\overline{F_{w_{OH}}}$ from refs. 19–21.

to the presence of polar hard segments and nonpolar soft segments.[2] Chen et al.[6] proposed schematic models depicting the microstructure evolution of the HTPB/toluene diisocyanate (TDI)/1,4-butanediol (BDO) polyurethane system, as a function of hard and soft segment content. Depending on segment contents, a phase inversion can occur and the continuous phase can be either soft or hard.

The present work concerns apparently quite different materials, urethane acrylate oligomers (PUA) based on HTPB. Because of the toxicity of free isocyanate in polyurethane formulation, one interest is to have formulation without isocyanate. One possibility is to replace the isocyanate end group by an acrylate group, followed by radical polymerization for curing and network formation. These acrylate precursors based on HTPB present the feature of having two types of reactive double bonds: acrylate and polybutadiene double bonds. The network structure is influenced by this parameter. But the particularity of the system used in this study is the structure and morphology of the precursor before radical polymerization. The aim of the present article is to observe, by SAXS, the degree of miscibility, and eventual phase-separation phenomena during precursor synthesis, the relationship between precursor structure, and morphology and other characteristics such as the effect of initial OH/NCO ratio on the amount of residual isocyanate, molar mass and molar mass distribution, crystallinity, glass-transition temperature (T_g), and viscosity (η). Morphologies and properties of the issued cured networks will be the subject of a further publication.

EXPERIMENTAL

Materials

The materials used in this study are listed in Table I. HTPB was dried under vacuum at 80°C for 6 h before use. All other reactants were used as received without any further purification.

Synthesis

Reactions in bulk and in high concentrated solution with methyl methacrylate (MMA) as the solvent were studied (Table II). A 500-mL four-necked flask equipped with a mechanical stirrer, nitrogen inlet, condenser, and addition funnel, heated in an oil bath at 80°C, was used for PUA synthesis.

A one-step synthesis procedure was used. For reactions in bulk, HTPB, 2-hydroxyethyl acrylate

Table II Nomenclature of Different Reactive Systems

Sample Name	Monomers	Synthesis Conditions
UA1B	HTPB/H_{12}MDI/HEA	In bulk
UA1S	HTPB/H_{12}MDI/HEA	In MMA
UA2B	HTPB/mTMXDI/HEA	In bulk
UA2S	HTPB/mTMXDI/HEA	In MMA
UA3B	HTPB/IPDI/HEA	In bulk
UA3S	HTPB/IPDI/HEA	In MMA
UA4B	HTPB/TDI/HEA	In bulk
UA4S	HTPB/TDI/HEA	In MMA

(HEA), hydroquinone (HQ), and dibutyl dilaurate (DBTL) were introduced into the flask until complete stabilization of the temperature, [HQ]/[acrylate] = 10^{-3} and [DBTL]/[isocyanate] = 5.10^{-4}. The diisocyanate was then added. A small decrease in the reactant temperature (typically 2°C) was observed before restabilization after 4 min. For reaction in solution, MMA (24 wt %) was added to alcohol monomers.

Apparatus

Infrared (IR) spectra were obtained using a Nicolet-550 FTIR spectrometer at room temperature. Final precursors were directly placed between KBr cells for analysis. Isocyanate conversion was estimated with the isocyanate peak area ($\bar{\nu}$ = 2269 cm^{-1}) to a reference peak area ratio ($\bar{\nu}$ = 2915 cm^{-1}, CH).

SAXS experiments were performed with a setup including a rotating anode X-ray generator with copper target, a point collimation produced mainly by two orthogonal mirrors, and a line position-sensitive proportional counter connected to a computer. The scattered intensity, I, was obtained as a function of the scattering vector $q = (4\pi/\lambda)\sin\theta$. The scattering vector range is $0.01 < q < 0.15$ $Å^{-1}$ and 2θ is the scattering angle in radian. The X-ray wavelength was 1.54 Å (Cu K_α radiation). The acquisition time was 60 min. The reactive mixture was placed in a cell (10-mm diameter, 1-mm thickness), protected by polyimide films (Kapton®). This cell was placed in a temperature-controlled system in order to conduct the precursor synthesis *in situ* and to measure the evolution of diffusion.

Different parameters can be obtained from SAXS curves. First, the Guinier theory describes the behavior for lower q values when interactions between diffusing domains are sharp. The equation has the form[22]

$$I(q) = I_0 \exp\left(-\frac{q^2 R_G^2}{3}\right) \quad (1)$$

where I is the scattered intensity, I_0 is a preexponential factor, q is the magnitude of scattering vector, and R_G is the Guinier radius or gyration radius.

The Porod theory describes the behavior for higher q values when interfaces are not fractal. The equation has the form[22]:

$$I(q) \sim \frac{A}{q^4} \quad (2)$$

where A is proportional to the area of diffusing particles.

Polarized optical microscopy (POM) was used to observe crystallization of precursors. POM was a Leica Laborlux 12 POLS. Size exclusion chromatography (SEC) measurements were made using Waters 510, with a refractive index detector. Columns of Polymer Laboratories gel 500 Å and 100 Å were used for the analysis of small molar mass products and 3 Millipore microstyragel HR1, HR2, and HR3 columns for analysis of high molar mass polymers. Molar masses were calculated using calibration with polystyrene standards. The solvent medium was tetrahydrofuran and was used at a 1 mL/min flow rate and a pressure of 3.10^3 Pa. Diphenyl (DP) was used as an internal standard for the measurement of diisocyanate conversion and percentage of the obtained diurethane acrylate.

Differential scanning calorimetry (DSC) measurements were carried out by using a Mettler TA300 instrument, operated at a 10°C/min heating rate. Sample masses of ~ 10 mg were used for these experiments. Dynamic mechanical tests for viscosity determinations were carried out, in shear mode, using a Rheometrics RSA II, with a cone plate (25-mm diameter) at various frequencies (γ = 0.1 to 100 s^{-1}), and at different temperatures. Molecular modeling was realized using Sybyl 6.3 program from the Tripos Company.

RESULTS AND DISCUSSION

Precursor Morphology

As the average functionality of HTPB is >2, the reaction with a diisocyanate could produce gela-

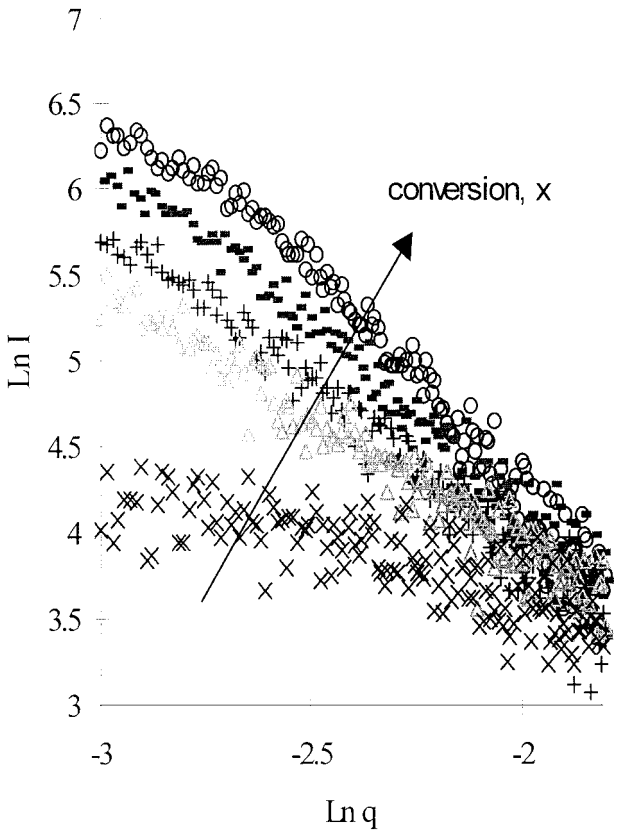

Figure 1 Scattering curves obtained for different conversions (×) during the precursor synthesis (UA1B) (×) $x = 0$; (△) $x = 0.60$; (+) $x = 0.70$; (○) $x = 0.97$.

tion of the reactive system depending on stoichiometric conditions and hydroxy or isocyanate conversion. Stoichiometric conditions were first chosen, according to Chen et al.,[23] to avoid gelation at full conversion. Stoichiometric conditions are as follows:

$$[OH]_{HTPB}/[NCO]/[OH]_{HEA} = 0.5/1/0.5$$

$$r = \frac{[OH]_0}{[NCO]_0} = 1 \text{ and } r' = \frac{[OH]_{HEA}}{[OH]_{HTPB}} = 1$$

After the first experiments, stoichiometric ratios were slightly modified (Table III). Reasons for this choice will be given below.

For reactions in bulk with these last stoichiometric ratios, SAXS experiments show the existence of scattered intensity. In Figure 1, $\ln(I)$ versus $\ln(q)$ is plotted for different conversions (x). At the beginning ($x = 0$), weak diffusion was observed, characteristic of small molecules (H_{12}MDI and HEA) homogeneously dispersed in HTPB prepolymer. After reaction, $x > 0.5$ (measured by IR), the scattered intensity becomes characteristic of dispersed particles and increases with conversion, meaning an increase in the surface area, A of the particles, according to Porod theory.[22] For $x = 1$, the slope value of the Porod diagram is equal to -3 different from -4, meaning that the scattering particles' outline is not well defined. These particles are characterized by an interphase or a fractal outline.[24] No correlation peak was observed, meaning that there is weak organization of particles. By contrast, when $\ln I$ is plotted versus q^2 (Guinier diagram, Fig. 2), we observe that diffusing particles always have the same Guinier radius (R_G), independent of the conversion of the reaction: all curves present identical slopes, proportional to R_G. These particles are compact and can be reasonably assumed to be assembling of hard segments. These hard segments could be diisocyanate reacted with two acrylates called diurethane acrylate (DUA) and HTPB diisocyanate-acrylate chain ends. Therefore, the alcohol-isocyanate reaction-induced phase separation is attributable to the immiscibility between such hard and soft segments and the soft polybutadiene chains.

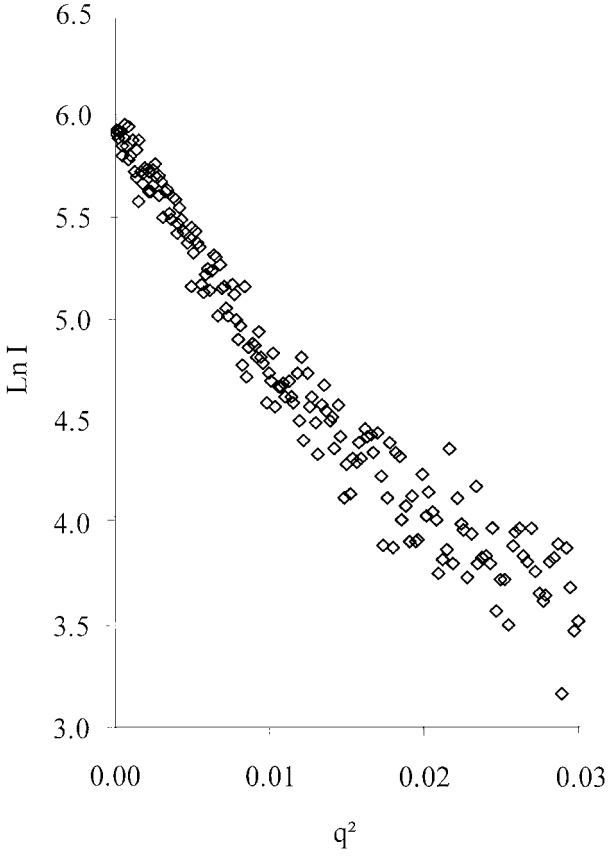

Figure 2 Guinier diagram for UA1B sample.

After a full reaction (UA1B, Fig. 2; UA2B, Fig. 3; UA3B, Fig. 4; UA4B, Fig. 5), all SAXS experiments on different systems with different diisocyanate show the presence of dispersed particles (Table III) and similar results. We observe that Guinier radii are independent of the type of the diisocyanate: $14 < R_G < 19$ Å. If we suppose that hard phases are organized as short sticks assembly (sticks are supposed to be infinitely thin), the length of assembly could be calculated by

$$L = \frac{2}{\sqrt{3}} R_G$$

Like the Guinier radius, length of assembling present little variations with the diisocyanate used: $48 < L < 66$ Å (Table III). These lengths are coherent with DUA lengths ($1_{max} \approx 20$ Å) determined by molecular modeling: assembling could reasonably be composed primarily of diurethane of acrylate molecules.

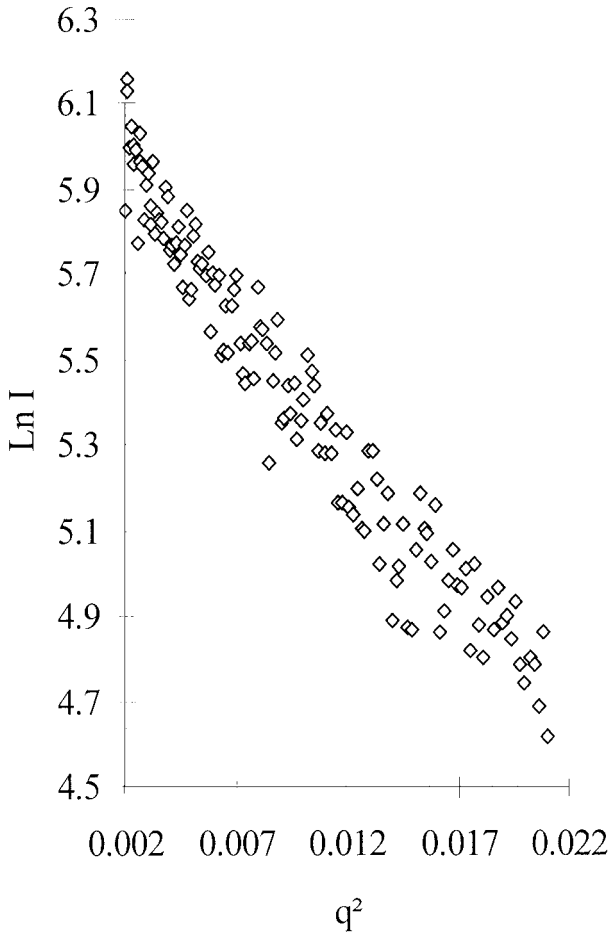

Figure 3 Guinier diagram for UA2B sample.

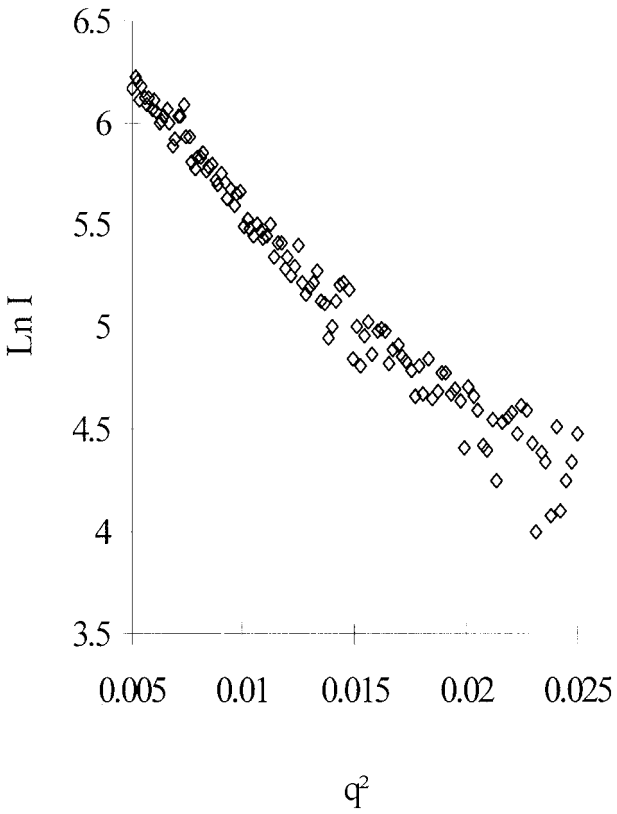

Figure 4 Guinier diagram for UA3B sample.

Such lengths can be compared with the results published by Etienne et al.,[7] who studied the structure of amorphous segmented polyurethanes based on hydrogenated polybutadiene, MDI, and neopentyl glycol as the chain extender. Using SAXS, these investigators observed domains of 50–150-Å size, comparable to heterogeneities of the size of precursors obtained in this study (Table III).

These morphological results can explain why the use of initial stoichiometric ratios 0.5/1/0.5 always led to the observation of unreacted isocyanate groups (Table IV). The incomplete reaction results when some isocyanate groups are "trapped" or "buried" in hard domains, in a reaction conducted at 80°C. For precursor synthesis in solution (in MMA), the solvent improves miscibility; as a result, no or few NCO functions are still unreacted at the end (Table IV).

One aim of this study was to prepare precursors without unreacted isocyanate in order to prevent secondary reactions such as urea formation. Seen that precursor synthesis in bulk at stoichiometric condition (0.5/1/0.5) generally leaded to residual isocyanate, OH/NCO ratios higher than

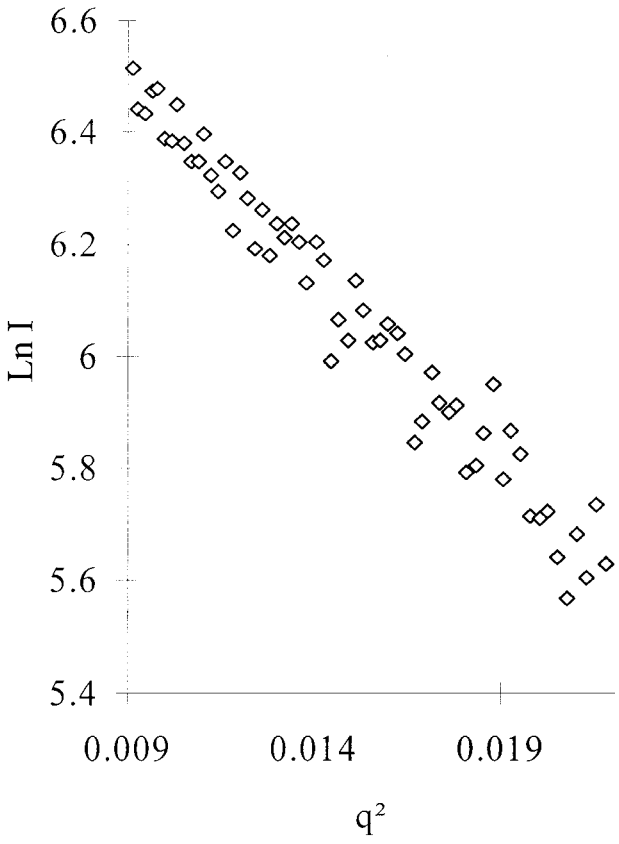

Figure 5 Guinier diagram for UA4B sample.

one were used. Complete isocyanate conversion was obtained with the stoichiometries presented in Table III; thus, they were used in the rest of this study.

Precursor Properties

Structure

All the following results are obtained with precursors synthesized using stoichiometric conditions noted in Table III. During precursor synthesis,

Table III Stoichiometric Conditions Leading to Complete Isocyanate Conversion and Corresponding SAXS Results

Sample	HTPB/Diisocyanate/HEA (in Functions)	R_G (Å)	L (Å)
UA1B	0.66/1/0.5	18.5	64
UA2B	0.7/1/0.5	14.0	48
UA3B	0.56/1/0.5	19.5	67
UA4B	0.60/1/0.5	14.5	50

R_G, Guinier or gyration radius; L, length of assembly.

Table IV Unreacted Isocyanate Functions for the Synthesis in Bulk and in Solution With the Same Stoichiometric Conditions ($[OH]_{HTPB}/[NCO]/[OH]_{HEA}$ = 0.5/1/0.5, in Functions

	% Unreacted NCO Groups	
Sample	Bulk	Solution
UA1	15	5
UA2	7	5
UA3	3	3
UA4	10	3

some chain extensions of the initial HTPB prepolymer occur depending on the stoichiometric ratio and the reactivities of the hydroxyl and isocyanate groups. Many investigators have studied the structure of HTPB. There are three types of OH group: hexene-2 ol-1 (H), vinylic (V), and geraniol (G) in different concentrations (H > V > G) and with different reactivities (G > H > V).[25–29] These three types of OH group are also in competition with the primary alcohol of HEA. In addition, the reactivities also depend on the type of isocyanate used for synthesis and different rate constants are reported in literature.[30–36] The phase-separation process during synthesis introduces another unknown parameter: the real concentrations of functional groups in soft and hard phases. As shown in Table V, products with different molar masses, molar mass distributions, and diurethane acrylate percentages were obtained. All these differences were expected as result of the complexity of the systems used. When MMA was used as a solvent, the conditions were again modified and the resulting products were also different.

In all experiments, HEA end-capped diisocyanate molecules are present. The presence of these DUA influences the structure of the precursor and will influence the structure of the final network obtained by radical-chain polymerization. The amount of DUA varies depending on diisocyanate structure and on the synthesis conditions (Table V); synthesis in solution leads to a higher percentage of diurethane acrylate.

Crystallization, Heterogeneities, and Thermal Properties

For some precursors, a melting peak was observed (Table VI). This peak could be related to

Table V Characteristics of Synthesized Precursors

Sample	Overall $\overline{M_w}$ (g/mol)	HTPB-Based Part		% Diurethane Acrylate (w/w)	Viscosity at 60°C (Pa/s)
		$\overline{M_w}$ (g/mol)	Ip		
UA1B	35,110	46,770	3,0	4	120
UA1S	47,850	67,100	4,8	7	
UA2B	32,580	41,810	3,4	5	28
UA2S	30,870	39,890	3,7	9	
UA3B	24,910	31,670	2,9	4	55
UA3S	33,390	47,700	3,6	8	
UA4B	44,240	59,870	3,5	11	54
UA4S	40,400	55,440	4,6	15	

$\overline{M_w}$ are expressed in PS standard. For initial HTPB the molar masses expressed in the same way: $\overline{M_w}$ = 9770 g/mol and $\overline{M_n}$ = 3840 g/mol. Stoichiometric conditions are defined in Table III for synthesis in bulk and are 0.5/1/0.5 for synthesis in solution.

the presence of the DUA molecules. The crystallites, structured in spherulites, can be observed by polarized optical microscopy (Fig. 6). Their diameters are around 0.4 mm. Comparing melting enthalpies (Tables VI and VII) shows that precursor enthalpies per gram of DUA are higher than those of pure diurethane acrylate. An explanation could be that crystallites are not pure, and entities other than DUA, such as the urethane acrylate chain ends of HTPB, are included in crystallites. The presence of heterogeneities observed by SAXS in amorphous precursors and spherulites in crystallized precursors is coherent with the possibility that crystallization of hard domains nucleates from the heterogeneities present in the amorphous precursors.

Table VI Thermal Properties of Synthesized Precursors

Sample	T_m (°C)	ΔH (J/g_{DUA})	$T_{g\ onset}$ (°C)[a]	ΔCp (J/g_{HTPB} K)[a]
UA1B	57.0	155	−85.2	0.64
UA1S	52.5	28.6	−77.5	0.27
UA2B	—	—	−80.1	0.39
UA2S	—	—	−83.4	0.53
UA3B	—	—	−82.4	0.47
UA3S	—	—	−82.5	0.62
UA4B	46.0	81.8	−82.9	0.70
UA4S	50.4	85.6	−74.1	0.59

[a] Glass-transition temperatures were measured after quenching to obtain amorphous prepolymers.

For precursors synthesized in solution, crystallites were also obtained after 3 or 4 months of storage at room temperature, whereas for precursor synthesized in bulk, they appeared after approximately 1 month of storage. Furthermore, enthalpies of precursors synthesized in solution (Table VI) are globally lower than enthalpies of precursors synthesized in bulk. As for the percentage of unreacted NCO, the results concerning the morphologies observed on a larger scale also depend on the synthesis conditions.

T_g (Table VI) is related to the HTPB-rich phase (the soft phase) ($T_{g\,HTPB}$ onset = −84.1°C). Heat capacities (ΔCp) at T_g of precursors were different from the ΔCp of initial HTPB [ΔCp_{HTPB} = 0.73 J/(g*K)]. This results from a modification of the molecular mobility of HTPB chains, depending on the environment. In fact, there is more affinity between diisocyanate-acrylate HTPB chain ends with DUA molecules than between pure HTPB chains, which leads to a decrease of HTPB chains molecular mobility.

In the case of solution synthesis (Table VI), T_g, and ΔCp measurements are disturbed by the crystallization of MMA (T_m = −48,2°C; ΔH = 111.8 J/g).

For both synthesis conditions, the T_g due to the diurethane acrylate-rich phase cannot be measured in precursors, even before crystallization (Table VII). Heat capacities due to the hard phase are too weak to be detected, probably because it is not a pure phase of DUA.

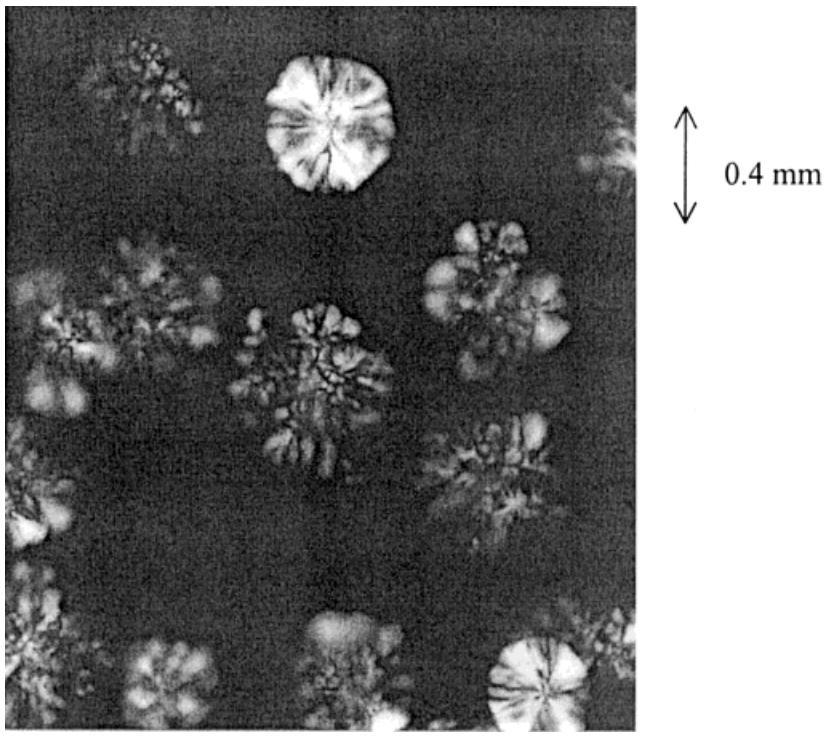

Figure 6 Observations of crystallites by POM (precursor UA1B).

Viscosity

Finally, precursor viscosities were measured at 60°C (Table V). All precursors exhibited Newtonian behavior. High values of viscosities are obtained compared with HTPB initial viscosity ($\eta_{HTPB,60°C}$ = 1.9 Pa/s).). These high viscosities are strongly induced by hydrogen bonds present in urethane groups.[37,38] These bonds take place between carbonyl (C═O) versus ether groups (COC) and on NH groups. The viscosity difference for the precursor obtained cannot be due to molar mass difference; it results from the complex structure of precursors, chain extension, microphase organization observed by SAXS, and the presence of crystallites for precursors based on H_{12}MDI (UA1B).

Table VII Thermal Properties of Pure Diurethane Acrylate

DUA Based on	T_m (°C)	ΔH (J/g)	$T_{g\ \text{onset}}$ (°C)[a]	ΔCp (J/g/K)[a]
H_{12}MDI (1)	—	—	−97.7[a]	0.87[a]
	54.3	24	−12.0[b]	0.29[b]
TDI (4)	—	—	−90.6[a]	0.78[a]
	58	42.7	−13.3[b]	0.53[b]

[a] Glass-transition temperatures were measured after quenching, to obtain amorphous molecules.

[b] Glass-transition temperatures of the amorphous phase of crystallized DUA.

CONCLUSIONS

Polyurethane acrylate precursors based on HTPB present the particularity of being organized on two scales:

1. Microphase separation was observed by SAXS during precursor synthesis, induced by the immiscibility between HTPB segments and urethane acrylate units. Hard microdomains (~ 50 Å in size) are composed principally of diurethane acrylate and urethane acrylate ends of HTPB.
2. Diurethane acrylate and urethane acrylate chain ends of HTPB present in the hard domains can crystallize.

These two levels of organization do not appear at the same time: microphase separation is observed during the precursor formation and crystallites can appear a long time after reaction (≥1

month). These results will be compared next with structures and properties of polyurethane acrylate networks.

ACKNOWLEDGMENTS

The authors thank Elf Atochem for supporting this work and F. Court for helpful discussions.

REFERENCES

1. Bonart, R. J Macrol Sci Phys 1968, B2, 115.
2. Cuvé, L.; Pascault, J. P.; Boiteux, G.; Seytre, G. Polymer 1991, 32, 343.
3. Van Bogart, J. W. C.; Gibson, P. E.; Cooper, S. L. J Polym Sci Phys 1983, 21, 65.
4. Gibson, P. E.; Van Bogart, J. W. C.; Cooper, S. L. J Polym Sci Phys 1986, 24, 885.
5. Leung, L. M.; Koberstein, J. T. J Polym Sci Phys 1985, 23, 1883.
6. Chen, C. H. Y.; Briber, R. M.; Thomas, E. L.; Xu, M.; MacKnight, W. J. Polymer 1983, 24, 1333.
7. Etienne, S.; Vigier, G.; Cuvé, L.; Pascault, J.-P. Polymer 1994, 35, 2737.
8. Lee, H. S.; Hsu, S. L. Macromolecules 1989, 22, 1100.
9. Yang, W. P.; Macosko, C. W. Makromol Chem Macromol Symp 1989, 25, 23.
10. Lee, H. S.; Wang, Y. K.; MacKnight, W. J.; Hsu, S. L. Macromolecules 1988, 21, 270.
11. Lin, S. B.; Hwang, K. S.; Tsay, S. Y.; Cooper, S. L. Colloid Polym Sci 1985, 263, 128.
12. Lee, H. S.; Wang, Y. K.; Hsu, S. L. Macromolecules 1987, 20, 2089.
13. Cuvé, L.; Pascault, J. P.; Boiteux, G. Polymer 1992, 33, 3957.
14. Kazmierczak, M. E.; Fornes, R. E.; Gilbert, R. D. J Polym Sci Phys 1989, 27, 2173.
15. Christenson, C. P.; Harthcock, M. A.; Meadows, M. D.; Spell, H. L.; Howard, W. L.; Creswick, M. W.; Guerra, R. E.; Turner, R. B. J Polym Sci Phys 1986, 24, 1401.
16. Ryan, A. J. Prog Rubber Plast Technol 1995, 11, 154.
17. Li, Y.; Gao, T.; Chu, B. Macromolecules 1992, 25, 1737.
18. Li, Y.; Ren, Z.; Zhao, M.; Yang, H.; Chu, B. Macromolecules 1993, 26, 612.
19. Wilkes, G. L.; Emerson, J. A. J Appl Phys 1979, 47, 4261.
20. Chen, C. H. Y.; Thomas, E. L.; MacKnight, W. J.; Schneider, N. S. Polymer 1986, 27, 659.
21. Li, C.; Goodman, S. L.; Albrecht, R. M.; Cooper, S. L. Macromolecules 1988, 21, 2367.
22. Glatter, O.; Kratky, O. Small-Angle X-Ray Scattering. Academic Press: London, 1982.
23. Chen, J.; Pascault, J.-P.; Taha, M. J Polym Sci Chem 1996, 34, 2889.
24. Schmidt, P. W. Modern Aspects of Small-Angle Scattering. Brumberger, H., Ed.; Chapter 1, Section 2.3. Kluwer Academic: Netherlands, 1995.
25. Pham, Q. T. Makromol Chem 1978, 179, 1011.
26. Descheres, I.; Paisse, O.; Ceccaldi, J. N. C.; Pham, Q. T. Makromol Chem 1987, 188, 538.
27. Descheres, I.; Pham, Q. T. Makromol Chem 1986, 187, 1963.
28. Allard Breton, B.; Audenaert, M.; Pham, Q. T. Macromol Chem Phys 1996, 197, 1651.
29. Ramao, M.; Scaariah, K. J.; Ravindra, P. V.; Chaudrasekharan, G.; Alwan, S.; Satri, K. S. J Appl Sci 1993, 49, 435.
30. Di Giacomo, A. J Phys Chem 1985, 26, 301.
31. Case, L. C. J Polym Sci 1960, 48, 27.
32. Coutinho, F. M. B. J Appl Polym Sci Chem 1986, 24, 727.
33. Aranguren, M. I.; Williams, R. J. J. Polymer 1986, 27, 425.
34. Cunliffe, A. V.; Davis, A.; Wright, J. Polymer 1985, 65, 301.
35. Peebles, L. H. Macromolecules 1976, 7, 872.
36. Peebles, L. H. Macromolecules 1976, 29, 2695.
37. Boyarchuk, Y. M.; Rappoport, L. Y.; Nikitin, V. N.; Apukhine, N. P. Polym Sci USSR 1965, 7, 859.
38. Coleman, M. M.; Skrovanek, D. J.; Hu, J.; Painter, P. C. Macromolecules 1988, 21, 59.